

Thermohaline mixing in stars : solving the long-standing ^3He problem

Corinne Charbonnel^{1,2} and Nadège Lagarde¹

¹Geneva Observatory, University of Geneva
Chemin des Maillettes 51, 1290 Versoix, Switzerland
email: Corinne.Charbonnel@unige.ch, Nadege.Lagarde@unige.ch

²CNRS UMR 5572, Toulouse University
14, av.E.Belin, 31400 Toulouse, France

Abstract. Thermohaline mixing has been recently identified as the dominating process that governs the photospheric composition of low-mass bright giant stars (Charbonnel & Zahn 2007a). Here we present the predictions of stellar models computed with the code STAREVOL that takes into account this mechanism together with rotational mixing and atomic diffusion. We compare our theoretical predictions with recent observations and discuss how the corresponding yields for ^3He are compatible with the observed behaviour of this light element in our Galaxy.

Keywords. Hydrodynamics, instabilities, Stars: abundances, evolution, rotation, Galaxy: abundances

1. The “ ^3He problem”

The classical theory of stellar evolution predicts a very simple Galactic destiny to ^3He , dominated by a large production of this isotope by low-mass stars (Iben 1967; Rood 1972; Rood *et al.* 1976; Dearborn *et al.* 1996; Weiss *et al.* 1996). As a consequence, one expects a large increase of ^3He with time in the Galaxy with respect to its primordial abundance (e.g., Tosi 1996). However, the ^3He content of Galactic HII regions (Balser *et al.* 1994, 1999; Bania *et al.* 1997, 2002) is very similar to that of the Sun and solar system (Geiss & Reeves 1972; Geiss 1993, Mahaffy *et al.* 1998), and very close to the BBN value (Coc *et al.* 2004; Cyburt 2004; Serpico *et al.* 2004). This is the so-called “ ^3He problem” that could be resolved if only $\sim 10\%$ or less of the low-mass stars were releasing ^3He as predicted by classical stellar theory (Tosi 1998, 2000; Palla *et al.* 2000; Charbonnel 2002; Romano *et al.* 2003).

Charbonnel & Zahn (2007a) showed that thermohaline mixing drastically reduces the ^3He production in low-mass, low-metallicity stars. Simultaneously, this mechanism changes the surface carbon isotopic ratio as well as the abundances of lithium, carbon and nitrogen.

2. Stellar models including thermohaline convection, rotation-induced mixing, and atomic diffusion

Here we present the predictions of new stellar models computed with the code STAREVOL for solar metallicity and stellar masses between 1 and 4 M_{\odot} . Computations include the transport of chemical species in the radiative regions due to thermohaline instability, rotational mixing, and atomic diffusion. For thermohaline transport we use the diffusion coefficient advocated by Charbonnel & Zahn (2007a) based on Ulrich (1972) arguments for the aspect ratio of the salt fingers as supported by laboratory experiments

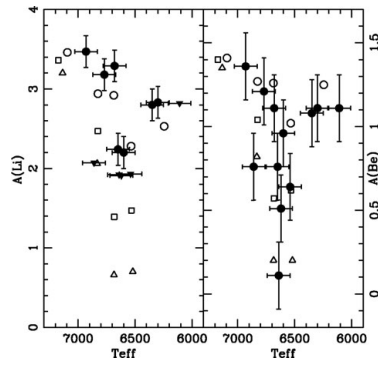


Figure 1. Li and Be abundances in IC 4651 main sequence and turnoff stars (black points and triangles for actual determinations and upper limits respectively). Open circles, squares, and triangles show model predictions for initial rotation velocities of 50, 80, and 110 km s⁻¹ respectively. On the cool side of the Li and Be dip the model with $T_{\text{eff}} \sim 6250$ K is from Talon & Charbonnel (2005) and takes into account additional transport of angular momentum by internal gravity waves. Adapted from Smiljanic *et al.* (2009b)

(Krishnamurti 2003) and on Kippenhahn *et al.* (1980) extended expression for the case of a non-perfect gas. The evolution of the internal angular momentum profile and the associated transport of chemicals are accounted for with the complete formalism developed by Zahn (1992) and Maeder & Zahn (1998) that takes into account advection by meridional circulation and diffusion by shear turbulence (see Palacios *et al.* 2003, 2006, and Decressin *et al.* 2009 for a description of the implementation in STAREVOL). Typical initial (i.e., ZAMS) surface rotation velocities are chosen for all the models depending on the stellar mass. We assume magnetic braking on the early main sequence for the stars with T_{eff} on the ZAMS lower than ~ 6900 K that have relatively thick convective envelopes (Talon & Charbonnel 1998). The adopted braking law follows the description of Kawaler (1988). Rotational velocity further decreases when the stars evolve on the subgiant branch due to radius expansion. Atomic diffusion is included in the form of gravitational settling as well as that related to thermal gradients, using the formulation of Paquette *et al.* (1986).

3. Model predictions for the surface abundances

The model predictions for the evolution of the surface abundances of various species have been validated all along the evolutionary sequence. They reproduce for example very nicely the surface abundances of Li and Be along the colour-magnitude diagram of the open cluster IC 4651 as shown in Fig.1 and 2. Note that thermohaline mixing is efficient only when RGB stars reach the so-called bump in the luminosity function, which is located at $T_{\text{eff}} \sim 4200$ K in the present case. For stars less evolved than the bump as those shown in both figures, the Li and Be behaviours are thus dictated by rotation-induced mixing (see Smiljanic *et al.* 2009b for more details and Smiljanic *et al.*, this volume; see also Charbonnel & Talon 1999 and Palacios *et al.* 2003).

Predictions for the evolution of the surface carbon isotopic ratio are shown in Fig. 3 for models of 1.25 and 2 M_{\odot} stars, and compared with observations in the open cluster M67 (turnoff mass $\sim 1.2 M_{\odot}$). We note that rotation-induced mixing on the main sequence slightly lowers the post-dredge-up $^{12}\text{C}/^{13}\text{C}$ value compared to the classical case (i.e., no rotation, diffusion, nor thermohaline mixing). At the luminosity of the bump ($\log(L/L_{\odot}) \sim 2$ for the 1.25 M_{\odot} star), thermohaline mixing leads to further decrease of

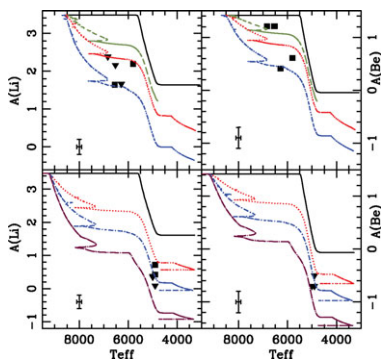


Figure 2. Li and Be abundances in IC 4651 evolved stars. Theoretical predictions for 1.8 and 2 M_{\odot} models are compared to observations of subgiant and giant stars (upper and lower panels respectively). Solid lines are for the classical case. Other lines correspond to different initial rotation velocities (80, 110, and 180 km s^{-1} for the 1.8 M_{\odot} star; 110, 180, and 250 km s^{-1} for the 2.0 M_{\odot} star). Adapted from Smiljanic *et al.* (2009b)

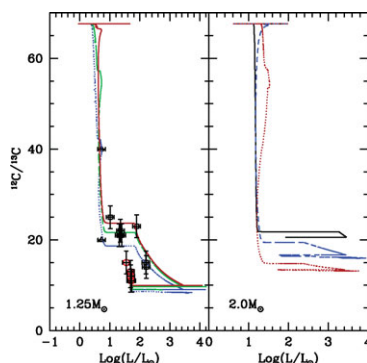


Figure 3. Evolution of the surface $^{12}\text{C}/^{13}\text{C}$ value as a function of stellar luminosity for models of 1.25 and 2 M_{\odot} stars (left and right panels respectively). Different tracks are for different initial rotation velocities (50, 80, and 110 km.s^{-1} for the 1.25 M_{\odot} star, and 0, 110, and 250 km.s^{-1} for the 2 M_{\odot} star). Observations by Gilroy & Brown (1991) in evolved stars of the open cluster M67 (turnoff mass $\sim 1.2 M_{\odot}$) are also shown (triangle, squares, and circles for subgiant, RGB, and clump stars respectively). Adapted from Lagarde & Charbonnel (in preparation)

the carbon isotopic ratio, in excellent agreement with M67 data. In the case of the 2 M_{\odot} star, thermal mixing becomes efficient at the bump in the luminosity function only when rotation in earlier phases is accounted for. Importantly we note that at solar metallicity, the $^{12}\text{C}/^{13}\text{C}$ values reached when thermal mixing ceases are higher than in the case of metal-poor stars where the carbon isotopic ratios almost always reach the equilibrium value (see Fig. 3 of Charbonnel & Zahn 2007a). This metallicity-dependence is in perfect agreement with the observational behaviour (see Fig. 1 of Charbonnel & Do Nascimento 1998).

In Fig. 4 we show the predictions for the $^{12}\text{C}/^{13}\text{C}$ surface ratio at the tip of the RGB and of the AGB for our models over the whole considered mass range and compare them with observations in stars belonging to open clusters of various turnoff masses. We see that in models for stars with masses below $\sim 1.7 M_{\odot}$, thermal mixing is the main physical process governing the photospheric composition of evolved giants, while rotation plays only a minor role on the red giant branch (see Palacios *et al.* 2006). In fact, the

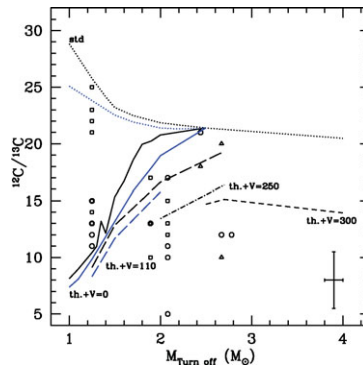


Figure 4. Theoretical predictions compared with observations of $^{12}\text{C}/^{13}\text{C}$ in open clusters spanning a large turnoff mass range. Data are from Smiljanic *et al.* (2009a) and Gilroy & Brown (1991). Squares, triangles and circles are for RGB, clump, and early-AGB stars respectively. Typical observational errors are indicated. Classical models (i.e., non-rotating and without thermohaline mixing) are shown as dotted lines. The solid lines are for models including thermohaline mixing only, while all the other models include rotation-induced mixing (with initial rotation velocities as indicated), thermohaline convection, and atomic diffusion. Black and blue lines correspond to model predictions at the tip of the RGB and AGB respectively. Adapted from Lagarde & Charbonnel (in preparation)

thermohaline diffusion coefficient at the RGB bump is several order of magnitudes higher than the total rotation-induced diffusion coefficient.

For more massive stars, thermohaline mixing occurs in the advanced phases when rotation-induced mixing is accounted for, but in a much less efficient manner. In this case, the final carbon isotopic ratio depends mainly on rotation-induced mixing on the main sequence that modifies the abundance profiles, and in particular the ^{13}C peak inside the stars, before the occurrence of the first dredge-up. Overall, the present models explain very well the observed abundance patterns over the considered mass range.

4. Model predictions for ^3He

On the main sequence, a ^3He peak builds up due to pp-reactions inside low-mass stars (Iben 1967), and is engulfed in the stellar envelope during the first dredge-up. As a consequence the surface abundance of ^3He strongly increases on the lower RGB as can be seen in Fig. 5 for various stellar masses. Its value reaches a maximum when the whole peak is engulfed. After the first dredge-up, the temperature at the base of the convective envelope is too low for ^3He to be nuclearly processed. As a result in canonical models this fresh ^3He is preserved until the ejection of the planetary nebula when it is released into the interstellar matter. This classical view is however contradicted by observations and chemical evolution models as discussed in § 1.

After the bump however, thermohaline mixing brings ^3He from the convective envelope down to the hydrogen-burning shell where it burns. This leads to a rapid decrease of the surface abundance (and thus of the corresponding yield) of this element as can be seen in Fig. 5, and as already shown by Charbonnel & Zahn (2007a) for low-metallicity stars. This confirms the early suggestion by Rood *et al.* (1984) that the variations of the carbon isotopic ratio and of ^3He are strongly connected (see also Charbonnel 1995; Charbonnel & Do Nascimento 1998; Eggleton *et al.* 2006). It is important to note that in the models presented here ^3He decreases by a large factor in the ejected material with respect to the canonical evolution predictions, but that low-mass stars remain net producers (while

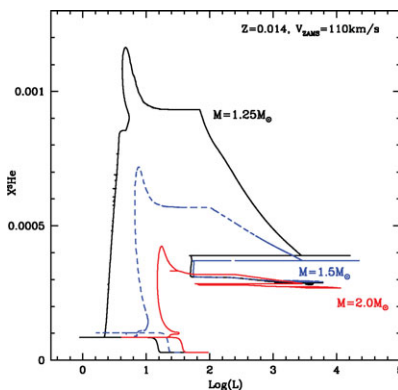


Figure 5. Evolution of the surface abundance of ^3He (in mass fraction) for stars of various initial masses and solar metallicity. Figure from Lagarde & Charbonnel (in preparation)

far much less efficient than in the canonical case) of ^3He . As already depicted by the $^{12}\text{C}/^{13}\text{C}$ behaviour that traces the dependance of the thermohaline mixing efficiency with metallicity, the destruction of fresh ^3He by this process is much more efficient in low-metallicity stars (see Fig. 4 of Charbonnel & Zahn 2007a).

Computations for a larger grid in stellar masses and metallicities are now being performed in order to quantify the actual contribution of low-mass stars to Galactic ^3He in the framework proposed here (Lagarde *et al.*, in preparation). We are confident that the corresponding ^3He yields will help reconciling the primordial nucleosynthesis with measurements of $^3\text{He}/\text{H}$ in Galactic HII regions (Charbonnel 2002).

5. The peculiar case of “thermohaline deviant stars”: Ap star descendants?

However a couple of planetary nebulae, namely NGC 3242 and J320, have been found to behave “classically” (see Bania, this volume): slightly more massive than the Sun, they are currently returning fresh ^3He to the interstellar medium, in the amount predicted by classical stellar models (Rood *et al.* 1992; Galli *et al.* 1997; Balser *et al.* 1999, 2006).

To reconcile the $^3\text{He}/\text{H}$ measurements in Galactic HII regions with the high values of ^3He in NGC 3242 and J320, Charbonnel & Zahn (2007b) proposed that thermohaline mixing is inhibited by a fossil magnetic field in RGB stars that are descendants of Ap stars. They obtained a threshold for the magnetic field of 10^4 – 10^5 Gauss, above which it inhibits thermohaline mixing in red giant stars located at or above the L-bump. Fields of that order are expected in the descendants of Ap stars, taking into account the contraction of their core when they become red giants.

Charbonnel & Zahn (2007b) thus concluded that in a large fraction of descendants of Ap stars thermohaline mixing does not occur. As a consequence these objects should produce ^3He as predicted by the standard stellar theory and as observed in the planetary nebulae NGC 3242 and J320. The relative number of such stars with respect to non-magnetic objects that undergo thermohaline mixing is consistent with the statistical constraint coming from observations of the carbon isotopic ratio in red giant stars (Charbonnel & Do Nascimento 1998). It satisfies also the Galactic requirements for the evolution of the ^3He abundance.

Acknowledgements

We acknowledge financial support from IAU, from the French “Programme National de Physique Stellaire” of CNRS/INSU, and from the Swiss National Science Foundation.

References

- Balser, D. A., Bania, T. M., Brockway, C. J., Rood, R. T., & Wilson, T. L., 1994, *ApJ*, 430, 667
- Balser, D. A., Bania, T. M., Rood, R. T., & Wilson, T. L., 1999, *ApJ*, 510, 759
- Balser, D. A., Goss, W. M., Bania, T. M., & Rood, R. T., 2006, *ApJ*, 640, 360
- Bania, T. M., Balser, D. A., Rood, R. T., Wilson, T. L., & Wilson, T. J., 1997, *ApJS*, 113, 353
- Bania, T. M., Rood, R. T., & Balser, D. A., 2002, *Nature*, 415, 54
- Charbonnel, C. 1995, *ApJ*, 453, L41
- Charbonnel, C. 2002, *Nature*, 415, 27
- Charbonnel, C. & Do Nascimento, J. D. 1998, *A&A*, 336, 915
- Charbonnel, C. & Talon, S. 1999, *A&A*, 351, 635
- Charbonnel, C. & Zahn, J. P. 2007a, *A&A Letters*, 467, L15
- Charbonnel, C. & Zahn, J. P. 2007b, *A&A Letters*, 476, L29
- Coc, A., Vangioni-Flam, E., Descouvemont, P., Adahchour, A., & Angulo, C. 2004, *ApJ*, 600, 544
- Cybur, R. H. 2004, *Phys. Rev.D*, 70, 023 505
- Dearborn, D. S. P., Steigman, G., & Tosi, M., 1996, *ApJ*, 465, 887
- Decressin, T., Mathis, S., Palacios, A., *et al.* 2009, *A&A*, 495, 271
- Eggleton, P. P., Dearborn, D. S. P., & Lattanzio, J. C 2006 *Science*, 314, 5805, 1580
- Galli, D., Stanghellini, L., Tosi, M., & Palla, F. 1997, *ApJ*, 477, 218
- Geiss, J. & Reeves, H., 1972, *A&A* 18, 126
- Geiss, J., 1993, in *Origin and evolution of the elements*, eds. N. Prantzos *et al.*, p. 89
- Gilroy, K. K. & Brown, J. A. 1991, *ApJ*, 371, 578
- Iben, I., 1967, *ApJ*, 143, 642
- Kawaler, S. D., 1988, *ApJ*, 333, 236
- Kippenhahn, R., Ruschenplatt, G., & Thomas, H. C. 1980, *A&A*, 91, 175
- Krishnamurti, R. 2003, *J. Fluid Mech.*, 483, 287
- Maeder, A. & Zahn, J. P. 1998, *A&A*, 334, 1000
- Palacios, A., Charbonnel, C., Talon, S., & Forestini, M. 2003, *A&A*, 399, 603
- Palacios, A., Charbonnel, C., Talon, S., & Siess, L. 2006, *A&A*, 453, 261
- Palla, F., Bachiller, R., Stanghellini, L., Tosi, M., Galli, D., 2000, *A&A*, 355, 69
- Paquette, C., Pelletier, C., Fontaine, G., & Michaud, G., 1986, *ApJS*, 61, 177
- Rood, R. T., 1972, *ApJ*, 177, 681
- Rood, R. T., Steigman, G., & Tinsley, B. M., 1976, *ApJ*, 207, L57
- Rood, R. T., Bania, T. W., & Wilson, T. L. 1984, *ApJ*, 280, 629
- Rood, R. T., Bania, T. W., & Wilson, T. L. 1992, *Nature*, 355, 618
- Romano, D., Tosi, M., Matteucci, F., & Chiappini, C. 2003, *MNRAS*, 346, 295
- Smiljanic, R., Gauderon, R., North, P., Barbuy, B., Charbonnel, C., & Mowlavi, N. 2009a, *A&A* 502, 267
- Smiljanic, R., Pasquini, L., Charbonnel, C., & Lagarde, N. 2009b, *A&A*, in press, astro-ph 0910.4399
- Talon, S. & Charbonnel, C 1998, *A&A*, 335, 959
- Talon, S. & Charbonnel, C 2005, *A&A*, 440, 981
- Tosi, M. 1996, *ASP Conference Series*, Vol. 98, 299
- Tosi, M. 1998, *Space Science Reviews*, Vol. 84, 207
- Tosi, M. 2000, *IAUS* 198, 525
- Ulrich, R. K. 1972, *ApJ*, 172, 165
- Weiss, A., Wagenhuber, J., & Denissenkov, P. A., 1996, *A&A*, 313, 581
- Zahn, J. P. 1992, *A&A*, 265, 115